Fatih Güleç[1,*]
Emir Hüseyin Şimşek[2,*]
Hilal Tanıker Sarı[2]

Prediction of Biomass Pyrolysis Mechanisms and Kinetics: Application of the Kalman Filter

In order to predict the pyrolysis mechanisms of four different biomasses (Asbos (*Psilocaulon utile*), Kraalbos (*Galenia africane*), Scholtzbos (*Pteronia pallens*), and palm shell), a novel method called Kalman filter was investigated and the results were compared by regression analysis. Both analyses were applied to five different generalized biomass pyrolysis models consisting of parallel and serial irreversible-reversible reaction steps. The models consisting of reversible reactions in addition to parallel pyrolysis steps demonstrated a better fit with the experimental results. The pyrolysis step from biomass to bio-oil has the highest reaction rates compared with the other pyrolysis steps defined in the models. The Kalman filter is thus defined as a promising filtering and prediction method for the estimation of detailed pyrolysis mechanisms and model parameters, using minimum experimental data.

Keywords: Biomass, Kalman filter, Pyrolysis, Pyrolysis models, Regression analysis

Received: May 26, 2021; *revised:* October 24, 2021; *accepted:* November 15, 2021

DOI: 10.1002/ceat.202100229

Supporting Information available online

1 Introduction

Biomass feedstocks are defined as clean, environmentally friendly, and inexpensive energy sources [1, 2]. Additionally, biomass feedstocks are also considered as CO_2-neutral energy sources since they are an integral part of the global carbon cycle [3, 4]. The different kinds of biomass therefore belong to the most promising feedstocks for the production of clean energy and fine chemicals using thermal (pyrolysis, combustion, hydrothermal) and biological process pathways [5–7]. However, there are several obstacles to the full commercialization of bioenergy and bioproducts via these technologies, including the resourcing of biomass, ineffective biomass refinery technologies, a lack of cost-competitive bioproducts, and a limited and/or unstable supply of biofuels and bioproducts. Furthermore, the differences in chemical and biological structures of biomass resources increase the obstacles to the commercialization of these technologies. Pyrolysis is one of the commonly used processes in which biomass can be effectively converted into more valuable and clean products: gas, liquid (bio-oil), and solid (bio-char) products [8–10]. In the pyrolysis process, the chemical bonds in the hemicellulose, cellulose, and lignin structures of the biomasses are thermally degraded in an oxygen-free environment. The pyrolysis process is usually categorized into three groups as "slow pyrolysis", "fast pyrolysis" and "flash pyrolysis", based on the heating rate, the temperature, and the residence time of the process conditions. To maximize the bio-char yield, a lower temperature (~400 °C) with a slower heating rate for a longer residence time (days) was suggested [11]. To maximize the gas yield, a higher temperature (650–1000 °C) with a higher heating rate for a shorter residence time (< 1 s), and finally, to maximize the liquid yield, an intermediate temperature (425–600 °C) with a higher heating rate (1000–10 000 °C s^{-1}) for a shorter residence time (< 3 s) were suggested [11]. Identifying the fundamental biomass pyrolysis mechanisms is, therefore, a challenge due to the differences in pyrolysis conditions and biomass structures.

Isoconversional methods, also called model-free methods, are the most popular methods for the kinetic analysis of biomass pyrolysis; they determine the activation energy using thermogravimetric analysis data [12, 13]. In these methods, the reaction model is the same at a specific conversion, regardless of the heating rate [13]. Furthermore, the reaction rate (degradation rate) can be determined by considering its temperature dependence according to the Arrhenius law. To identify the pyrolysis mechanism, the single-step global kinetic model "biomass → volatile gases + char" was proposed as an irreversible first-order pyrolysis mechanism, which is one of the widely used models [14–16]. However, the single-step global model has limitations in predicting all pyrolysis mechanisms due to the consideration of only primary reaction mechanisms [9], as pyrolysis reaction mechanisms could also include secondary

[1]Dr. Fatih Güleç
Fatih.Gulec1@nottingham.ac.uk
Department of Chemical Engineering, Faculty of Engineering, University of Nottingham, Nottingham NG7 2RD, UK.
[2]Dr. Emir Hüseyin Şimşek, Hilal Tanıker Sarı
Emir.Simsek@eng.ankara.edu.tr
Department of Chemical Engineering, Faculty of Engineering, Ankara University, 06100 Ankara, Turkey.

 © 2021 Wiley-VCH GmbH

reactions such as bio-oil degradation to gas or polymerization of bio-oils to bio-char [17, 18]. Therefore, the pyrolysis reaction was modified with additional secondary interactions, as the primary reaction runs through with parallel reactions ("virgin biomass → volatile + gas and virgin biomass → char") and the products in the primary reactions give second interactions ("$(\text{volatile} + \text{gas})_1 + (\text{char})_1 \rightarrow (\text{volatile} + \text{gas})_2 + (\text{char})_2$") [19, 20]. After demonstrating the importance of secondary reactions, the studies on detailed lumped kinetic models received more attention [21, 22]. Cuoci et al. [22] suggested lumped kinetic models for the biomass devolatilization and investigated the kinetics for each type of biomass structure of hemicellulose, cellulose, and lignin, with 15 reactions under 30 lumped species. Additionally, a detailed mechanistic study was investigated for the devolatilization and gas-phase reaction of the gases released through the thermal decomposition of biomass based on three reference components, by Ranzi et al. [21], to describe the biomass pyrolysis mechanism.

Although understanding the reaction mechanisms is of utmost importance for process optimization and reactor design, the measurement techniques fall short of all the variables in these kinds of dynamic processes [23–25]. It is also relatively difficult to experimentally investigate the reversibility of the pyrolysis reactions, while it may be one of the crucial steps for a better definition of the biomass pyrolysis reactions. However, recent findings in computational modeling stand out as a great solution for the identification of these kinds of reaction mechanisms and for validation of the modeling results with the experimental findings [26–29]. In previous studies, a group of different coal liquefaction mechanisms, which consists of reversible and irreversible steps, were suggested for a variety of different coals, and the most promising liquefaction mechanisms were clarified and determined using the Kalman filter method, which has recently become an attractive technique used in chemical reactions, with the validation of experimental results [26–29].

The aim of the study described in this manuscript is to understand the pyrolysis mechanisms and kinetics of four different biomass feedstocks (Asbos (*Psilocaulon utile*), Kraalbos (*Galenia africane*), Scholtzbos (*Pteronia pallens*), and palm shell) by using a novel filtering method: the Kalman filter. This is the first study that demonstrates the applicability of the Kalman filter to the prediction of the mechanisms and kinetics of the proposed biomass pyrolysis models. Based on this, five different generalized pyrolysis models consisting of reversible and irreversible steps were proposed to predict the pyrolysis mechanisms of these biomasses with the Kalman filter and regression analysis. The validity of the proposed models is determined by the sum of the squared differences of the values calculated with the models and experimental data.

2 Experimental Method and Pyrolysis Models

2.1 Experimental Data

The experimental biomass pyrolysis data that were used in the discrete-time models in this study were produced by De Jongh et al. [30] who investigated the vacuum pyrolysis of Asbos (*P. utile*), Kraalbos (*G. africane*), and Scholtzbos (*P. pallens*) at 450 °C for 30, 60, and 90 min, and by Abnisa et al. [31] who investigated the fast pyrolysis of palm shell at 500 °C for 30, 60, 90, 120, and 150 min. The pyrolysis products (i.e., bio-char, bio-oil, and gas) are presented in Appendix A Tab. A1 of the Supporting Information. These experimental data were used to validate the proposed models and investigate the pyrolysis kinetics by application of the Kalman filter and regression analysis.

2.2 Proposed Pyrolysis Mechanisms

A number of pyrolysis models consisting of serial and parallel steps have been published to identify the biomass pyrolysis processes with different properties [32–34]. Five different biomass pyrolysis models based on lumped parameters of bio-oil (liquid, B) and gas (C) were investigated for the pyrolysis of the four different biomasses feedstocks: Asbos (*P. utile*), Kraalbos (*G. africane*), Scholtzbos (*P. pallens*), and palm shell. The proposed biomass pyrolysis models have a group of parallel and serial irreversible-reversible reaction steps, as shown in Fig. 1. Model 1 illustrates a simplistic biomass pyrolysis mechanism involving the subsequent formation of liquid and gases from the thermal decomposition of biomass. Model 2 represents a reversible reaction between solid and liquid products in addition to Model 1. Contrary to the first two models, Model 3 consists of two parallel irreversible reactions where the liquid and gas products are simultaneously produced from the biomass. Model 4 presents an additional pyrolysis step from liquid to gas products in addition to the proposed pyrolysis Model 3. In addition to irreversible pyrolysis steps, reversible reaction steps by the polymerization of liquid products may also occur, due to trace amounts of transition metals. Therefore, Model 5 represents a reversible reaction between solid and liquid products in addition to the proposed pyrolysis process in Model 4. In the models, A, B, and C represent the remaining bio-char, bio-oil, and gas, respectively.

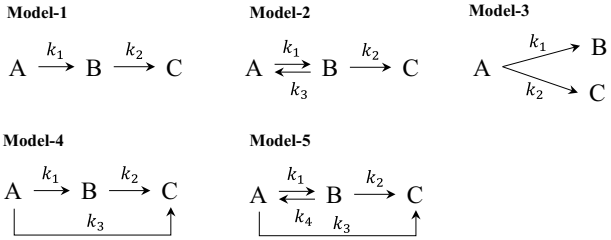


Figure 1. Proposed biomass pyrolysis models. A represents the biomass (or remaining char), B and C represent the pyrolysis products as bio-oil and gas, respectively.

The very early studies about biomass pyrolysis proposed that the decomposition rates of the biomass can be modeled based on the thermal behavior of the main components and their relative contributions to the chemical structure of the biomasses [35–38]. Biomasses can thermally decompose through breaking the chemical bonds in their molecules, producing a gas mixture

 © 2021 Wiley-VCH GmbH

rich in hydrocarbons, a bio-oil based liquid, and a solid (biochar) rich in carbon (as shown in the predicted models in Fig. 1). The produced fragments usually become smaller molecules; however, they may also combine to produce a residue with a larger molecular mass, or even an amorphous covalent solid. Therefore, the yields of these products and the pyrolysis mechanism mainly depend on the chemical composition of the raw biomass and the pyrolysis conditions such as the temperature, the heating rate, and the residence time. Biomasses may contain water, oxygen, and/or other substances, which may contribute to combustion, hydrolysis, or any other chemical process besides pyrolysis [39]. However, the adverse chemical reactions may be avoided by the application of an inert atmosphere or vacuum conditions. Additionally, pyrolysis in a vacuum atmosphere may decrease the boiling point of the by-products, which improves their recovery [40, 41].

The current reaction steps accepted for biomass pyrolysis assume that the volatiles (including some moisture) are evaporated below 100 °C [42]. Additionally, heat-sensitive substances such as proteins may partially decompose at this stage. When the pyrolysis temperature reaches around 100–120 °C, the remaining moisture is removed from the material, but higher temperatures are required to remove the water trapped in the crystal structure of hydrates. For example, sugars in the biomass structures start decomposing at 160–180 °C, with some condensable chemicals starting decomposition in a very early stage of the pyrolysis, which leads to parallel pyrolysis mechanisms as suggested in Models 3–5 instead of serial steps. Additionally, the organic molecules (fats, waxes, sugars, etc.) break down at temperatures between 100 and 500 °C [42]. Additionally, the main biomass structures such as hemicellulose, cellulose, and lignin also demonstrate thermal decomposition trends at about 220–315 °C, 315–400 °C, and 160–900 °C, respectively [43–45].

A large number of volatile organic compounds and non-condensable gases (H_2, CH_4, C_nH_m, CO, CO_2, and N) may be released from the biomass processed by pyrolysis [46–48]. Some of the volatiles may ignite and burn to create a visible flame. The solid residue from the pyrolysis of the biomasses is generally described as "bio-char", having a high carbon content with a color ranging from brown to black. The char also consists of ash and trace amounts of metals such as Na, K, Hg, Cd, Be, Se, Sb, As, Pb, Zn, Cr, Co, Ni [49–51], which may catalyze the pyrolysis reaction with an additional cracking reaction [52–54], supporting a serial reaction from bio-oil to gases as suggested in Models 1, 2, 4, and 5. On the other hand, free radicals may polymerize and produce high-molecular-weight products [28, 29, 55], as suggested in the reversible steps in Models 2 and 5. It is known that biomass-based waxes consist of a group of chemicals including *n*-alkanes, branched-chain alkanes, alkenes, esters, free fatty acids, primary and secondary fatty alcohols, aldehydes, ketones, and many others [53, 56]. In the presence of oxygen, some of the carbonaceous and nitrogen-containung residues may oxidize at about 200–300 °C with no (or little) visible flame, and thus the combustion gases CO, CO_2, and NO_x are released [57]. Furthermore, other elements such as sulfur, chlorine, and arsenic may also be oxidized at this stage.

2.3 Kalman Filter Method

The Kalman filter, also known as linear quadratic estimation, is an iterative mathematical process that uses a set of equations and consecutive data inputs to estimate the unknown variables in a process, which tends to be more precise than methods based on a single measurement [58–61]. The Kalman filter can be used to predict the unknown parameters using the known parameters of the period with the minimum variance of state variables, by using the three main stages of filtering, smoothing, and prediction [60, 62]. The Kalman filter operates in two steps; first, the current state of the variables is estimated, along with their uncertainties in the prediction step. Second, once the output of the next measurement is obtained, these estimates are updated using a weighted average, with more weight being given to estimates with higher certainty [28]. Therefore, the reaction rate constants of the complex biomass pyrolysis models can be predicted using the Kalman filter method. Further information about the Kalman filtering theory and its application in the prediction of kinetic parameters of different chemical processes using MATLAB has been presented in previous studies [26–29].

The compliance of the proposed pyrolysis models with the experimental data is figured out by forming first-order [63] linear discrete-time models [29, 55, 64]. Additionally, the reaction rate constants for each of the reactions in the models are determined using a MATLAB program (written in ver. 7.11; The MathWorks Inc., Natick, MA, USA) with the use of the Kalman filter. The discrete-time models and reaction rate equations are provided in Eqs. (1)–(3) and Eqs. (4)–(6) as an example of Model 5[1)] The reaction rate equations for the Models 1–4 are provided in Appendix B of the Supporting Information.

$$C_{A(i+1)} = C_{Ai}(1 - (k_1 + k_3)\Delta t) + k_4 C_{Bi}\Delta t \quad (1)$$

$$C_{B(i+1)} = C_{Bi} + (k_1\, C_{Ai} - (k_2 + k_4)C_{Bi})\Delta t \quad (2)$$

$$C_{C(i+1)} = C_{Ci} + (k_3 C_{Ai} + k_2 C_{Bi})\Delta t \quad (3)$$

where C_A is the unreacted biomass yield (wt %), C_B and C_C are the liquid and gas product yields (wt %), respectively, and k_1 to k_4 are the reaction rate constants for each reaction.

For Model 5:

$$\frac{dA}{dt} = -(k_1 + k_3)A + k_4 B \quad (4)$$

$$\frac{dB}{dt} = k_1 A - (k_2 + k_4)B \quad (5)$$

$$\frac{dC}{dt} = k_2 B + k_3 A \quad (6)$$

1) List of symbols at the end of the paper.

 © 2021 Wiley-VCH GmbH

2.4 Regression Analysis Method

Regression analysis is a method used to determine the relationship between at least two variables [65]. It not only determines the model of the relationship between variables but also makes predictions for an unknown variable by using the known variables and investigates the strength of the relationship between these variables [65–68]. In the regression analysis using the SigmaPlot program (ver. 12.0 Notebook, Systat Software, Inc.), as the first step, the equation giving the lowest error rate with the experimental results for the biomasses is found as a cubic expression (Eq. (8)). The coefficients of Eq. (8) were determined and are presented in Appendix A Tab. A2 of the Supporting Information. The derivative of this equation gives the reaction rate equation (Eq. (9)). The reaction rate equations of Model 5 are presented in Eqs. (10)–(12). The reaction rate equations for Models 1–4 are provided in Appendix B of the Supporting Information.

General regression equation:

$$y = a + bx \tag{7}$$

$$Y = y_0 + at + bt^2 + ct^3 \tag{8}$$

$$\frac{dY}{dt} = a + 2bt + 3ct^2 \tag{9}$$

where y is the dependent variable, a, b, and c are regression coefficients, and x is the independent variable.

For Model 5:

$$\frac{dA}{dt} = -k_1 A^m - k_3 A^n + k_4 B^p \tag{10}$$

$$\frac{dB}{dt} = k_1 A^m - k_2 B^r - k_4 B^p \tag{11}$$

$$\frac{dC}{dt} = k_3 A^n + k_2 B^r \tag{12}$$

The best model explaining the pyrolysis of the selected biomasses is defined by the sum of the squared differences of the values, calculated with the models and experimental data, using Eq. (13) [28].

$$\sum_i \left(y_{m_i} - y_{e_i}\right)^2 = (l_m - l_e)^2 + (g_m - g_e)^2 \tag{13}$$

Where y_{mi} and y_{ei} are the values calculated from the model and the experimental data, l_m and l_e are the liquid yields, and g_m and g_e are the gas yields calculated using the model and the experimental data, respectively.

3 Results and Discussion

3.1 Determination of the Pyrolysis Kinetics with the Kalman Filter

The findings from the models by forming the first-order linear discrete-time models with the application of the Kalman filter are compared with the experimental data supplied for Asbos (*P. utile*), Kraalbos (*G. africane*), Scholtzbos (*P. pallens*), and palm shell, and the results are presented in Figs. 2–6. Additionally, the reaction rate constants for each of the reactions in the proposed models and the sum of the squared differences of the values calculated with the models and experimental data are shown in Tab. 1. In Model 1, the biomass is first converted to liquids (B), which can also be defined as bio-oil, and then gases (C) are produced from the bio-oils in a serial reaction pathway. It is assumed that the pyrolysis of biomass would cause the scission of the bonds in a specific way [55]. Therefore, first, a group of fragments, which is defined as liquid bio-oil, would be produced during the thermal decomposition of the biomass. The other assumption in Model 1 is that the non-condensable

Table 1. Sums of the squared differences of the values calculated with the models and experimental data for four different biomasses and reaction rate constants (min^{-1}) for the models.

Biomass	Model	$\sum_i \left(y_{m_i} - y_{e_i}\right)^2$	Reaction rate constants $[min^{-1}] \times 10^3$			
			k_1	k_2	k_3	k_4
Asbos (*P. utile*)	1	4.51	0.65	6.08	–	–
	2	4.07	5.97	5.54	16.75	–
	3	3.75	0.55	2.32	–	–
	4	3.63	0.88	5.33	0.92	–
	5	3.08	3.98	3.74	1.57	15.31
Scholtzbos (*P. pallens*)	1	6.65	3.95	8.07	–	–
	2	6.36	11.26	7.60	16.09	–
	3	4.56	1.28	0.14	–	–
	4	4.37	1.68	0.09	0.01	–
	5	3.98	8.21	0.38	0.32	16.15
Kraalbos (*G. africane*)	1	7.07	4.98	8.67	–	–
	2	6.88	15.83	7.59	14.86	–
	3	4.06	0.95	3.62	–	–
	4	4.17	0.50	5.29	2.01	–
	5	3.85	9.34	1.73	6.04	15.38
Palm shell	1	6.83	1.22	0.96	–	–
	2	6.41	21.91	0.75	1.37	–
	3	4.66	0.26	0.83	–	–
	4	4.56	0.12	0.11	1.11	–
	5	4.87	13.49	0.35	4.75	10.96

 © 2021 Wiley-VCH GmbH

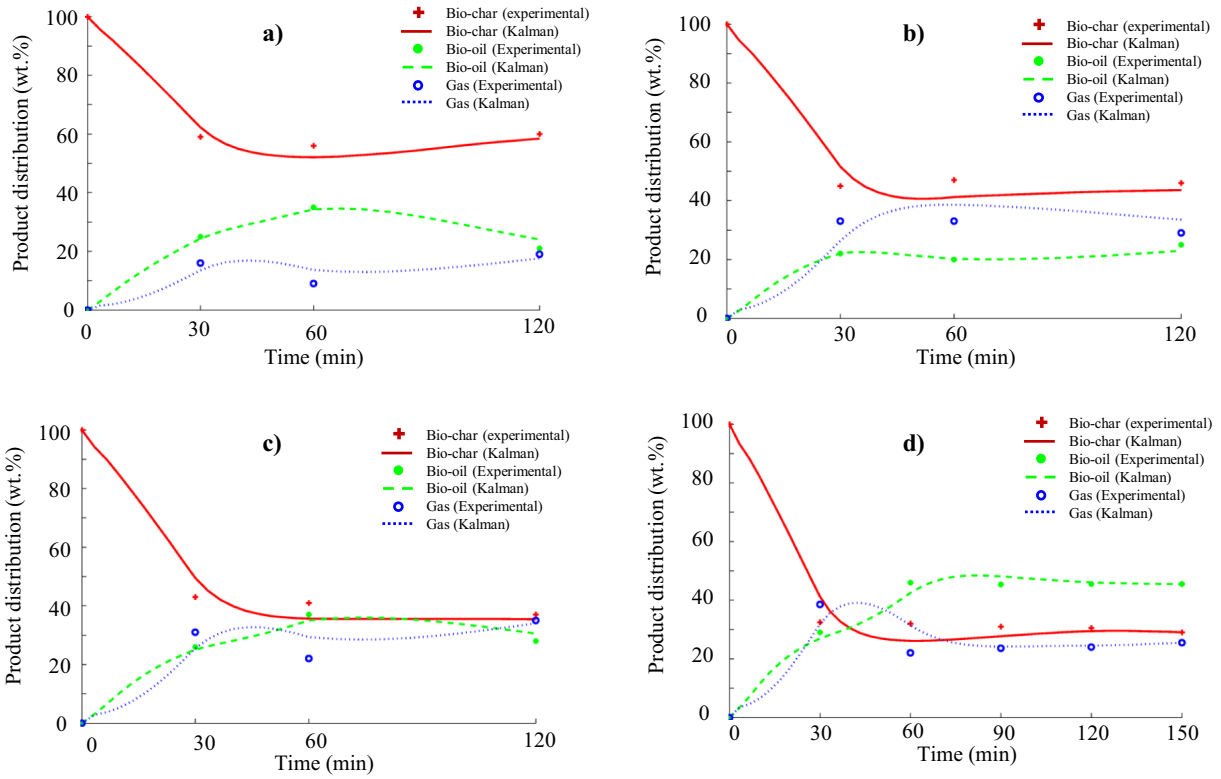


Figure 2. Comparison of Model 1 with the experimental data for (a) Asbos (*P. utile*), (b) Scholtzbos (*P. pallens*), (c) Kraalbos (*G. africane*), and (d) palm shell.

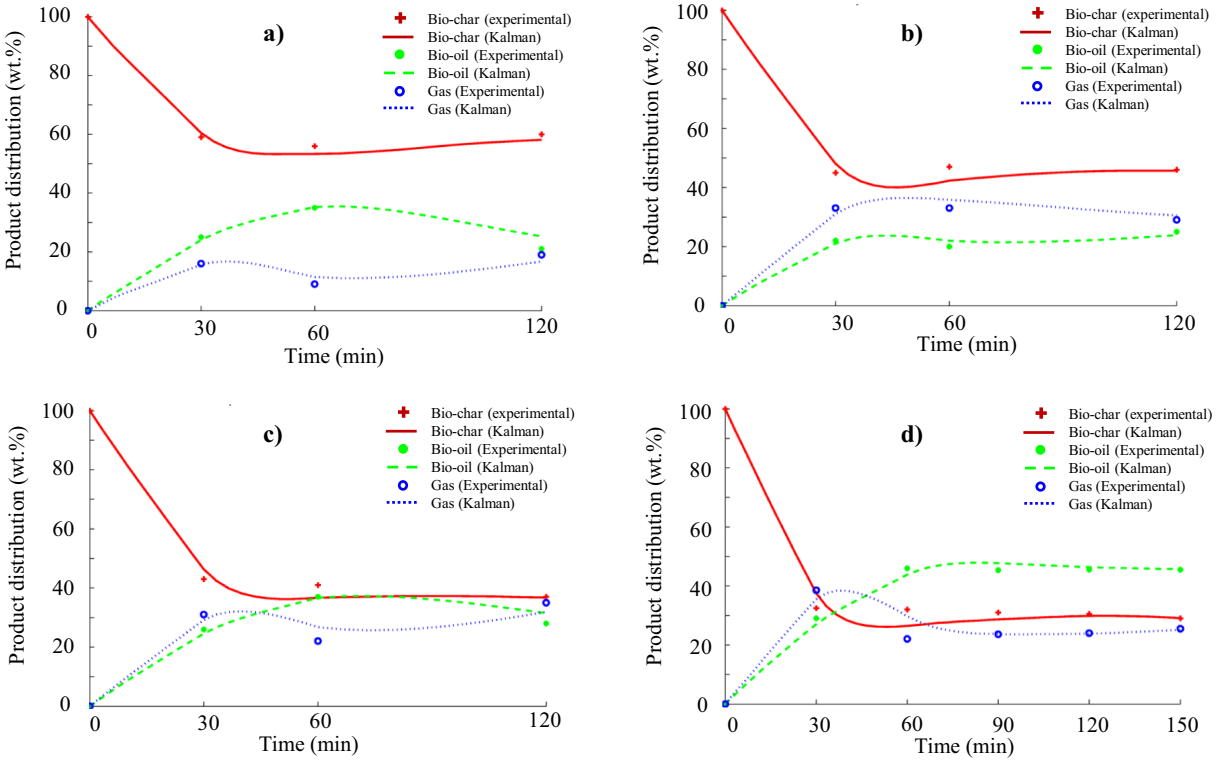


Figure 3. Comparison of Model 2 with the experimental data for (a) Asbos (*P. utile*), (b) Scholtzbos (*P. pallens*), (c) Kraalbos (*G. africane*), and (d) palm shell.

 © 2021 Wiley-VCH GmbH

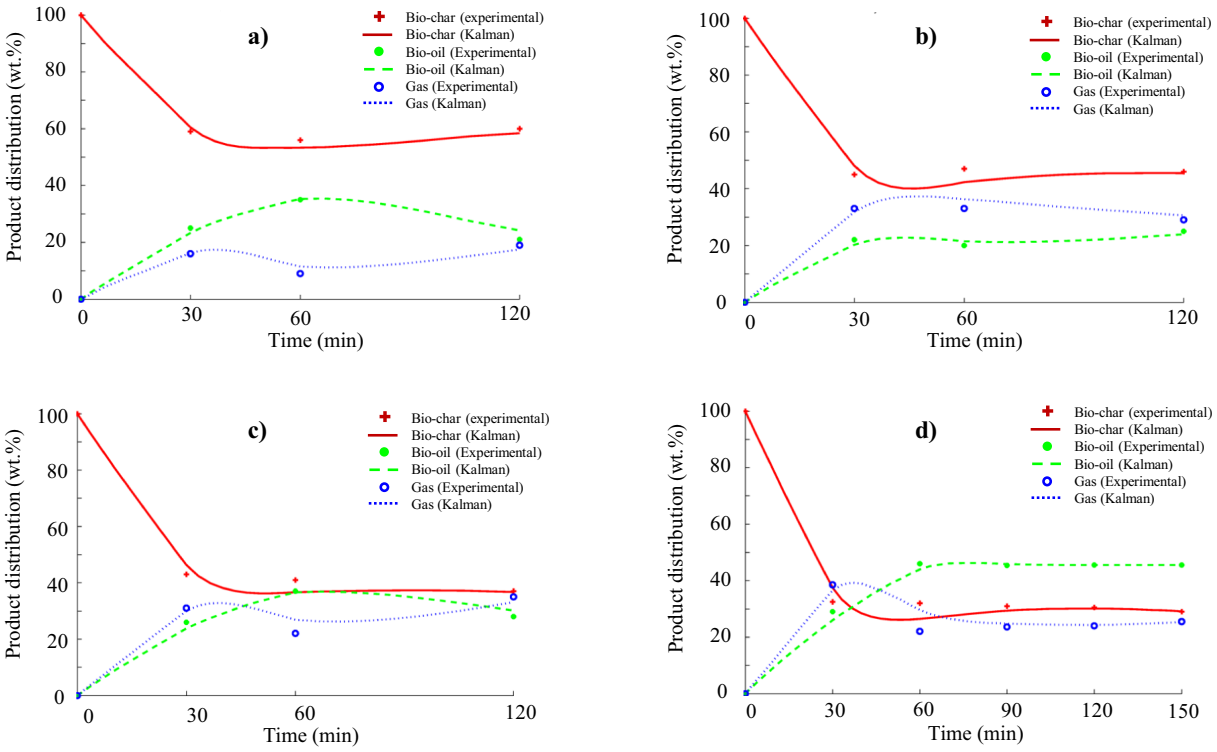


Figure 4. Comparison of Model 3 with the experimental data for (a) Asbos (*P. utile*), (b) Scholtzbos (*P. pallens*), (c) Kraalbos (*G. africane*), and (d) palm shell.

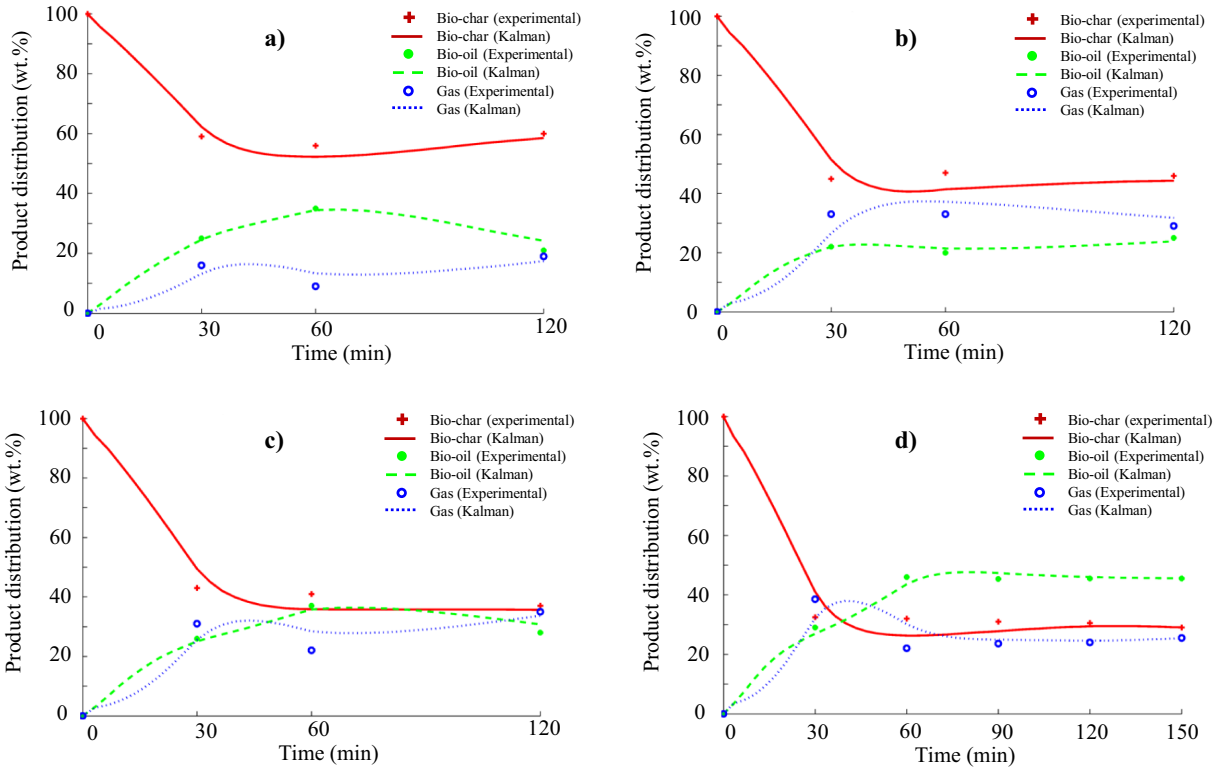


Figure 5. Comparison of Model 4 with the experimental data for (a) Asbos (*P. utile*), (b) Scholtzbos (*P. pallens*), (c) Kraalbos (*G. africane*), and (d) palm shell.

 © 2021 Wiley-VCH GmbH

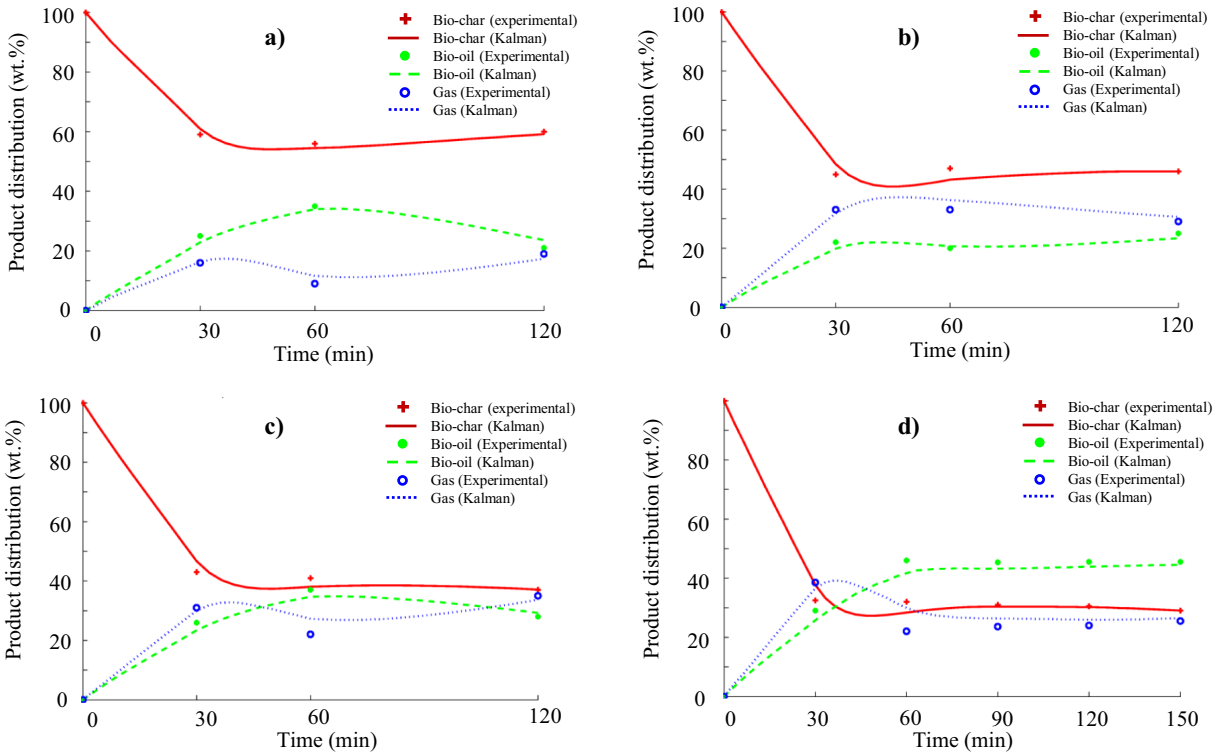


Figure 6. Comparison of Model 5 with the experimental data for (a) Asbos (*P. utile*), (b) Scholtzbos (*P. pallens*), (c) Kraalbos (*G. africane*), and (d) palm shell.

gases (i.e., H_2, CH_4, CO, CO_2, and N) are formed by the thermal or catalytic cracking of the liquid bio-oil.

In addition to Model 1, Model 2 represents a reversible reaction between the bio-char and bio-oils (bio-char ↔ bio-oils) under the assumption of polymerization of the free radicals in the liquid products. The sums of the squared differences obtained by comparison of Model 1 and Model 2 with the experimental data demonstrate that these models cannot fully describe the biomass pyrolysis, as demonstrated in Tab. 1. The incompatibility of Model 1 (Fig. 2) and Model 2 (Fig. 3) with the experimental data proves that the gas products may arise from biomass rather than from bio-oil.

The experimental results demonstrate that both the gas and liquid yields were gradually increased in the first 30 min of the pyrolysis of Asbos (*P. utile*), Scholtzbos (*P. pallens*), Kraalbos (*G. africane*), and palm shell. Therefore, the models having parallel pyrolysis reactions from biomass (A) to bio-oil (B) and gas (C) would be expected to demonstrate a better explanation for the pyrolysis of these biomasses, as proposed in Model 3. Fig. 4 (Model 3) shows the importance of the parallel reactions, biomass to bio-oil and biomass to gas, for the definition of the biomass pyrolysis, as the model shows better fit with the experimental data compared with Model 1 and Model 2.

In addition to these parallel reactions, the formation of gases may also be contributed by the cracking of bio-oils over the trace metals in the biomass, as metals such as Cu, Co, Mn, and Fe may contribute to the pyrolysis reaction with cracking reactions [52, 54, 69]. The experimental data demonstrates that, although the formation of bio-oil continues to increase, the formation of gas slightly decreases after 60 min for the pyrolysis of Asbos (*P. utile*) and Kraalbos (*G. africane*). Subsequently, a decrease in the bio-oil yield was observed after 120 min, with an increase in the gas and/or char yields. The increase in the gas yield may be attributed to the cracking of the bio-oils by the catalytic effects of trace amounts of metals. Therefore, Model 3 is updated with an additional reaction step from bio-oil to gases, as presented in Model 4. Furthermore, the increase in bio-char may also be attributed to the polymerization of free radicals. A large number of free radicals can be formed by the cracking of hydrocarbons thanks to the beta-scission reaction, which breaks the carbon-carbon bond. The free radicals may polymerize and produce high-molecular-weight products in the absence of hydrogen, which demonstrates an additional reversible reaction step of biomass ↔ bio-oils, as presented in Model 5.

As demonstrated in Figs. 5 and 6, in Models 4 and 5 the formation of bio-oil and gas products from direct biomass pyrolysis better fits with the experimental data supplied from the pyrolysis of all four biomasses. Furthermore, the sum of the squared differences (Tab. 1) supports this fitting and the importance of the reversibility between bio-char and bio-oil. Model 5 represents the best fitting with the experimental data for the vacuum pyrolysis of Asbos (*P. utile*), Scholtzbos (*P. pallens*), and Kraalbos (*G. africane*) compared with the other models, as shown in Fig. 5. Model 4 demonstrates the best fitting with the experimental data for the fast pyrolysis of palm shell compared with the other models, as demonstrated in Fig. 6. Furthermore, the sum of the squared differences illustrated in Tab. 1 also

 © 2021 Wiley-VCH GmbH

proves that Model 4 and Model 5 provide the best prediction for biomass pyrolysis, compared with the other three models.

The kinetic results for Model 5 (Tab. 1) demonstrate that the reaction rate from biomass → bio-oil (k_1) is much higher than the reaction rate from biomass → gas (k_3) for the pyrolysis of these biomasses, similar to the experimental data in which the formation of bio-oil was faster than the formation of gas. The highest reaction rates for the pyrolysis step of biomass → bio-oil for Asbos (*P. utile*), Scholtzbos (*P. pallens*), Kraalbos (*G. africane*), and palm shell were determined as 3.9×10^{-3}, 8.2×10^{-3}, 9.3×10^{-3}, and $13.5\times10^{-3}\,\mathrm{min}^{-1}$, respectively. Furthermore, the reaction rate for the reversible step from bio-oil to bio-char (presented in Model 5) was found as $1.5\times10^{-2}\,\mathrm{min}^{-1}$ for the vacuum pyrolysis of Asbos (*P. utile*), Scholtzbos (*P. pallens*), and Kraalbos (*G. africane*) and as $1.1\times10^{-2}\,\mathrm{min}^{-1}$ for the fast pyrolysis of palm shell.

3.2 Determination of the Pyrolysis Kinetics with Regression Analysis

The reaction rates and orders were determined by regression analysis for the best three models defined by the Kalman filter, and the results are presented in Tab. 2. Although Model 5 does not provide a better fit in the regression analysis, Models 3 and 4 presented a relatively low sum of the squared differences with the experimental data collected by the vacuum pyrolysis of Asbos, Scholtzbos, and Kraalbos, and the fast pyrolysis of palm shell. The reaction rates from biomass → bio-oil (k_1) and biomass → gas (k_3) were calculated as much higher than the reaction rate from bio-oil → gas (k_2) in Model 4. This may be attributed to the formation of gas run through direct biomass pyrolysis with a small contribution by bio-oil cracking, as the reaction order (p) for this step was also much lower than in the other pyrolysis steps, as presented in Tab. 2. On the other side, a relatively high reaction order for the main pyrolysis steps (from biomass to bio-oil or gas) was determined, as presented in Tab. 2. The varying reaction orders resulted from the differences in the biomass. In Model 3, the reaction orders for the pyrolysis step from biomass → gas (n) were determined as about 3.5 for Kraalbos, 2.8 for Scholtzbos, and 2.2 for palm shell, which are roughly 1.6–1.1 times higher than for the pyrolysis step from biomass → bio-oil (m).

4 Conclusion

Models 3, 4, and 5, where the products are formed from biomass in parallel pyrolysis reactions, show a better fit with the experimental data compared with Models 1 and 2, proposing pyrolysis in a series of reactions by the Kalman filter and regression analysis. However, the Kalman filter provided a better estimation for the biomass pyrolysis reaction kinetics compared to regression analysis. Model 5 was the best one of the proposed models; it consists of reversible reaction steps in addition to parallel pyrolysis steps, with the assumption of

Table 2. Sums of the squared differences of the values calculated with the models and experimental data for four different biomasses and reaction rate constants (mass fraction$^{(1-n)}$min^{-1}) for the models.

Biomass	$\sum_i (y_{m_i} - y_{e_i})^2$	Reaction rate constants [mass fraction$^{(1-n)}$min^{-1}]				Reaction orders			
Models		k_1	k_2	k_3	k_4	m	n	p	r
Asbos (*P. utile*)									
Model 3	6.74	1.2×10^{-8}	1.2×10^{-7}	–	–	4.0	3.4	–	–
Model 4	6.71	6.9×10^{-10}	7.6×10^{-17}	1.2×10^{-7}	–	4.6	3.4	0.6	–
Model 5	49.53	2.4×10^{-26}	2.0×10^{-2}	1.6×10^{-7}	8.6×10^{-3}	1.6	1.7	1.3	0
Scholtzbos (*P. pallens*)									
Model 3	13.03	9.7×10^{-6}	3.4×10^{-6}	–	–	2.5	2.8	–	–
Model 4	13.17	7.1×10^{-2}	5.1×10^{-17}	3.4×10^{-6}	–	0.6	2.8	0	–
Model 5	13.17	7.1×10^{-2}	3.5×10^{-18}	3.4×10^{-6}	9.5×10^{-16}	0.6	2.8	0	0
Kraalbos (*G. africane*)									
Model 3	22.30	5.7×10^{-5}	1.6×10^{-7}	–	–	2.2	3.5	–	–
Model 4	23.12	3.6×10^{-1}	6.6×10^{-24}	7.5×10^{-7}	–	0.2	3.2	0.4	–
Model 5	1000<	3.2×10^{-1}	1.0×10^{-17}	1.6×10^{-7}	4.5×10^{-6}	1.6	3.5	1.3	0.6
Palm shell									
Model 3	14.80	5.0×10^{-4}	5.4×10^{-5}	–	–	1.7	2.2	–	–
Model 4	14.68	4.8×10^{-5}	4.4×10^{-20}	5.5×10^{-5}	–	2.3	2.2	0	–
Model 5	1000<	3.5×10^{-1}	2.7×10^{-16}	5.4×10^{-5}	3.0×10^{-4}	2.2	0	2.2	0

 © 2021 Wiley-VCH GmbH

first-order linear discrete-time models. The highest reaction rates for the pyrolysis of Asbos, Scholtzbos, Kraalbos, and palm shell were found as 3.9×10^{-3}, 8.2×10^{-3}, 9.3×10^{-3}, and $13.5\times10^{-3}\,\mathrm{min}^{-1}$, respectively, for the step from biomass → bio-oil. Although it is possible to generalize, the reaction rate constants and reaction orders are fully dependent on the biomass properties.

This study demonstrates that the Kalman filter is a promising filtering method to estimate the biomass pyrolysis models and parameters using minimum experimental data, as the most stable results were obtained with the Kalman filter. As future work, detailed studies on the mechanisms of biomass pyrolysis to value-added chemicals (products) could be made to identify the impact of pyrolysis conditions such as the residence time, the temperature, and the heating rate in a commercial pyrolysis process. Those detailed pyrolysis mechanisms must be investigated for specific types of biomass due to the differences in the physicochemical properties of biomass feedstocks.

Supporting Information

Supporting Information for this article can be found under DOI: https://doi.org/10.1002/ceat.202100229.

The authors have declared no conflict of interest.

Symbols used

a, b, c	[–]	regression coefficients in regression analysis
C_A	[wt %]	unreacted biomass yield
C_B	[wt %]	liquid product yields
C_C	[wt %]	gas product yields
g_m	[wt %]	gas yields determined by modeling
g_e	[wt %]	experimental gas yields
l_m	[wt %]	liquid yield determined by modeling
l_e	[wt %]	experimental liquid yield
k_1 to k_4	[min^{-1}]	reaction rate constants
y	[–]	dependent variable in regression analysis
y_{mi}	[wt %]	values calculated from the model data in the sum of the squared differences
y_{ei}	[wt %]	values calculated from the experimental data in the sum of the squared differences
x	[–]	independent variable in regression analysis

Subscripts

A	biomass
B	liquid products from pyrolysis
C	gas products from pyrolysis
e	experimental data
m	model data

References

[1] M. Kumar, A. O. Oyedun, A. Kumar, *Renewable Sustainable Energy Rev.* **2018**, *81*, 1742–1770. DOI: https://doi.org/10.1016/j.rser.2017.05.270

[2] E. T. Kostas, O. S. Williams, G. Duran-Jimenez, A. J. Tapper, M. Cooper, R. Meehan, J. P. Robinson, *Biomass Bioenergy* **2019**, *125*, 41–49. DOI: https://doi.org/10.1016/j.biombioe.2019.04.006

[3] K. Tekin, S. Karagöz, S. Bektaş, *Renewable Sustainable Energy Rev.* **2014**, *40*, 673–687. DOI: https://doi.org/10.1016/j.rser.2014.07.216

[4] F. Gulec, E. H. Simsek, A. Karaduman, *J. Fac. Eng. Archit. Gazi Univ.* **2016**, *313*, 610–621. DOI: https://doi.org/10.17341/gummfd.93160

[5] F. Güleç, L. M. G. Riesco, O. Williams, E. T. Kostas, A. Samson, E. Lester, *Fuel* **2021**, *302*, 121166. DOI: https://doi.org/10.1016/j.fuel.2021.121166

[6] Y. Shen, *Biomass Bioenergy* **2020**, *134*, 105479. DOI: https://doi.org/10.1016/j.biombioe.2020.105479

[7] G. Özsin, A. E. Pütün, E. Pütün, *Biomass Convers. Biorefin.* **2019**, *9 (3)*, 593–608. DOI: https://doi.org/10.1007/s13399-019-00390-9

[8] Q. Zhang, J. Chang, T. Wang, Y. Xu, *Energy Convers. Manage.* **2007**, *48 (1)*, 87–92. DOI: https://doi.org/10.1016/j.enconman.2006.05.010

[9] S. Hameed, A. Sharma, V. Pareek, H. Wu, Y. Yu, *Biomass Bioenergy* **2019**, *123*, 104–122. DOI: https://doi.org/10.1016/j.biombioe.2019.02.008

[10] N. Khuenkaeo, S. Phromphithak, T. Onsree, S. R. Naqvi, N. Tippayawong, *PLoS One* **2021**, *16 (7)*, e0254485. DOI: https://doi.org/10.1371/journal.pone.0254485

[11] P. Basu, *Biomass Gasification, Pyrolysis and Torrefaction: Practical Design and Theory*, Academic Press, New York **2018**.

[12] I. Ali, R. Tariq, S. R. Naqvi, A. H. Khoja, M. T. Mehran, M. Naqvi, N. Gao, *J. Energy Inst.* **2021**, *95*, 30–40. DOI: https://doi.org/10.1016/j.joei.2020.12.002

[13] S. A. Khan, I. Ali, S. R. Naqvi, K. Li, M. T. Mehran, A. H. Khoja, A. A. Alarabi, A. Atabani, *J. Anal. Appl. Pyrolysis* **2021**, *158 (9)*, 105149. DOI: https://doi.org/10.1016/j.jaap.2021.105149

[14] N. Prakash, T. Karunanithi, *J. Appl. Sci. Res.* **2008**, *4 (12)*, 1627–1636.

[15] N. Prakash, T. Karunanithi, *Asian J. Sci. Res.* **2009**, *1*, 1–27.

[16] M. J. Antal, G. Varhegyi, E. Jakab, *Ind. Eng. Chem.* **1998**, *37 (4)*, 1267–1275. DOI: https://doi.org/10.1021/ie970144v

[17] D. S. Scott, J. Piskorz, D. Radlein, *Ind. Eng. Chem. Process.* **1985**, *24 (3)*, 581–588.

[18] F. Thurner, U. Mann, *Ind. Eng. Chem. Process.* **1981**, *20 (3)*, 482–488.

[19] G. Varhegyi, M. J. Antal, Jr., E. Jakab, P. Szabó, *J. Anal. Appl. Pyrolysis* **1997**, *42 (1)*, 73–87.

[20] P. N. Sheth, B. V. Babu, in *Proceedings of the National Conference on Environmental Conservation 2006* (Eds: B. V. Babu, V. Ramakrishna), Pilani **2006**, 453–458.

[21] E. Ranzi, A. Cuoci, T. Faravelli, A. Frassoldati, G. Migliavacca, S. Pierucci, S. Sommariva, *Energy Fuels* **2008**, *22 (6)*, 4292–4300. DOI: https://doi.org/10.1021/ef800551t

 © 2021 Wiley-VCH GmbH

[22] A. Cuoci, T. Faravelli, A. Frassoldati, S. Granata, G. Migliavacca, S. Pierucci, E. Ranzi, S. Sommariva, in *Proc. of the 30th Meeting of the Italian Section of the Combustion Institute*, ASICI, Milan **2007**.

[23] C. Boztepe, A. Künkül, N. Gürbüz, I. Özdemir, *Int. J. Chem.* **2019**, *51 (12)*, 931–942. DOI: https://doi.org/10.1002/kin.21321

[24] C. Boztepe, A. Künkül, N. Gürbüz. *J. Mol. Struct.* **2020**, *1209*, 127948. DOI: https://doi.org/10.1016/j.molstruc.2020.127948

[25] C. Boztepe, M. Daskin, A. Erdogan, T. Sarici, *Polym. Eng. Sci.* **2021**, *61*, 2083–2096. DOI: https://doi.org/10.1002/pen.25736

[26] G. Welch, G. Bishop, *An Introduction to the Kalman Filter*, University of North Carolina at Chapel Hill, Chapel Hill, NC **2006**.

[27] M. Grewal, A. Andrews, *Kalman Filtering: Theory and Practice Using MATLAB*, John Wiley & Sons, New York **2001**.

[28] E. H. Şimşek, F. Güleç, H. Kavuştu, *Fuel* **2017**, *207*, 814–820. DOI: https://doi.org/10.1016/j.fuel.2017.06.004

[29] E. H. Şimşek, F. Güleç, H. Kavuştu, A. Karaduman, *J. Fac. Eng. Archit. Gazi Univ.* **2019**, *34 (1)*, 79–88. DOI: https://doi.org/10.17341/gazimmfd.416464

[30] W. A. De Jongh, M. Carrier, J. H. Knoetze, *J. Anal. Appl. Pyrolysis* **2011**, *92 (1)*, 184–193. DOI: https://doi.org/10.1016/j.jaap.2011.05.015

[31] F. Abnisa, W. W. Daud, W. Husin, J. Sahu, *Biomass Bioenergy* **2011**, *35 (5)*, 1863–1872. DOI: https://doi.org/10.1016/j.biombioe.2011.01.033

[32] A. Anca-Couce, *Prog. Energy Combust.* **2016**, *53*, 41–79. DOI: https://doi.org/10.1016/j.pecs.2015.10.002

[33] J. Blondeau, H. Jeanmart, *Biomass Bioenergy* **2012**, *41*, 107–121. DOI: https://doi.org/10.1016/j.biombioe.2012.02.016

[34] A. Sharma, V. Pareek, D. Zhang, *Renewable Sustainable Energy Rev.* **2015**, *50*, 1081–1096. DOI: https://doi.org/10.1016/j.rser.2015.04.193

[35] S. Ward, J. Braslaw, *Combust. Flame* **1985**, *61 (3)*, 261–269. DOI: https://doi.org/10.1016/0010-2180(85)90107-5

[36] C. Koufopanos, A. Lucchesi, G. Maschio, *Can. J. Chem. Eng.* **1989**, *67 (1)*, 75–84. DOI: https://doi.org/10.1002/cjce.5450670111

[37] P. T. Williams, S. Besler, *Fuel* **1993**, *72 (2)*, 151–159. DOI: https://doi.org/10.1016/0016-2361(93)90391-E

[38] J. Caballero, R. Font, A. Marcilla, *Thermochim. Acta* **1996**, *276*, 57–77. DOI: https://doi.org/10.1016/0040-6031(95)02794-7

[39] M. Balat, M. Balat, E. Kırtay, H. Balat, *Energy Convers. Manage.* **2009**, *50 (12)*, 3147–3157. DOI: https://doi.org/10.1016/j.enconman.2009.08.014

[40] M. Garcìa-Pèrez, A. Chaala, C. Roy, *J. Anal. Appl. Pyrolysis* **2002**, *65 (2)*, 111–136. DOI: https://doi.org/10.1016/S0165-2370(01)00184-X

[41] M. Garcia-Perez, A. Chaala, H. Pakdel, D. Kretschmer, C. Roy, *J. Anal. Appl. Pyrolysis* **2007**, *78 (1)*, 104–116. DOI: https://doi.org/10.1016/j.jaap.2006.05.003

[42] H. Zhou, Y. Long, A. Meng, Q. Li, Y. Zhang, *Thermochim. Acta* **2013**, *566*, 36–43. DOI: https://doi.org/10.1016/j.tca.2013.04.040

[43] M. Carrier, L. Auret, A. Bridgwater, J. H. Knoetze, *Energy Fuels* **2016**, *30 (10)*, 7834–7841. DOI: https://doi.org/10.1021/acs.energyfuels.6b00794

[44] H. Yang, R. Yan, H. Chen, D. H. Lee, C. Zheng, *Fuel* **2007**, *86 (11/12)*, 1781–1788. DOI: https://doi.org/10.1016/j.fuel.2006.12.013

[45] H. Zhou, Y. Long, A. Meng, S. Chen, Q. Li, Y. Zhang, *RSC Adv.* **2015**, *5 (34)*, 26509–26516. DOI: https://doi.org/10.1039/C5RA02715B

[46] F. Pinto, F. Paradela, F. Carvalheiro, L. C. Duarte, P. Costa, R. N. André, *Chem. Eng. Trans.* **2018**, *70*, 793–798. DOI: https://doi.org/10.3303/CET1870133

[47] M. N. Uddin, W. W. Daud, H. F. Abbas, *Renewable Sustainable Energy Rev.* **2013**, *27*, 204–224. DOI: https://doi.org/10.1016/j.rser.2013.06.031

[48] M. Shahbaz, A. AlNouss, P. Parthasarathy, A. H. Abdelaal, H. Mackey, G. McKay, T. Al-Ansari, *Biomass Convers. Biorefin.* **2020**, 1–13. DOI: https://doi.org/10.1007/s13399-020-01040-1

[49] Q. Qi, C. Sun, J. Zhang, Y. He, Y. W. Tong, *Chem. Eng. J.* **2021**, *406*, 126833. DOI: https://doi.org/10.1016/j.cej.2020.126833

[50] L. Abou Jaoude, P. Castaldi, N. Nassif, M. V. Pinna, G. Garau, *Sci. Total Environ.* **2020**, *711*, 134511. DOI: https://doi.org/10.1016/j.scitotenv.2019.134511

[51] J. Tang, C. Cao, F. Gao, W. Wang, *Environ. Technol. Innov.* **2019**, *16*, 100492. DOI: https://doi.org/10.1016/j.eti.2019.100492

[52] F. Güleç, W. Meredith, C.-G. Sun, C. E. Snape, *Energy* **2019**, *173*, 658–666. DOI: https://doi.org/10.1016/j.energy.2019.02.099

[53] T. Ahmad, M. Rafatullah, A. Ghazali, O. Sulaiman, R. Hashim, *J. Environ. Sci. Health C* **2011**, *29 (3)*, 177–222. DOI: https://doi.org/10.1080/10590501.2011.601847

[54] F. Güleç, W. Meredith, C.-G. Sun, C. E. Snape, *Chem. Eng. J.* **2020**, *389*, 124492. DOI: https://doi.org/10.1016/j.cej.2020.124492

[55] E. H. Simsek, F. Güleç, F. S. Akcadag, *Fuel Process. Technol.* **2020**, *198*, 106227. DOI: https://doi.org/10.1016/j.fuproc.2019.106227

[56] E. H. Sin, The extraction and fractionation of waxes from biomass, *Ph.D. Thesis*, University of York, York **2012**.

[57] H. Chen, Y. Wang, G. Xu, K. Yoshikawa, *Energies* **2012**, *5 (12)*, 5418–5438. DOI: https://doi.org/10.3390/en5125418

[58] R. E. Kalman, *J. Basic Eng.* **1960**, *82 (1)*, 35–45.

[59] G. Welch, G. Bishop, *An introduction to the Kalman filter*, Department of Computer Science University of North Carolina at Chapel Hill, Chapel Hill, NC **1995**, 27599–3175.

[60] R. J. Meinhold, N. D. Singpurwalla, *Am. Stat.* **1983**, *37 (2)*, 123–127.

[61] E. A. Wan, R. Van Der Merwe, in *Proceedings of the IEEE 2000 Adaptive Systems for Signal Processing, Communications, and Control Symposium* (Cat. No. 00EX373), IEEE, Lake Louise **2000**, 153–158.

[62] S. J. Julier, J. K. Uhlmann, in *Signal Processing, Sensor Fusion, and Target Recognition VI* (Ed: I. Kadar), vol. 3068, SPIE., Bellingham, WA **1997**, 182–193.

[63] G. Varhegyi, E. Jakab, M. J. Antal, Jr., *Energy Fuels* **1994**, *8 (6)*, 1345–1352.

 © 2021 Wiley-VCH GmbH

[64] F. Güleç, G. D. T. Özdemir, *Akademik Ziraat Dergisi* **2017**, *6 (1)*, 73–80.
[65] M. P. Allen, *Understanding Regression Analysis*, Springer Science & Business Media, Berlin **2004**.
[66] C. Lu, W. Song, W. Lin, *Biotechnol. Adv.* **2009**, *27 (5)*, 583–587. DOI: https://doi.org/10.1016/j.biotechadv.2009.04.014
[67] S. Chatterjee, A. S. Hadi, *Regression Analysis by Example*, John Wiley & Sons, New York **2015**.
[68] D. C. Montgomery, E. A. Peck, G. G. Vining, *Introduction to Linear Regression Analysis*, John Wiley & Sons, New York **2021**.
[69] F. Güleç, W. Meredith, C.-G. Sun, C. E. Snape, *Fuel* **2019**, *244*, 140–150. DOI: https://doi.org/10.1016/j.fuel.2019.01.168

 © 2021 Wiley-VCH GmbH